JMEPEG (2005) 14:709-716
DOI: 10.1361/105994905X75493

©ASM International
1059-9495/$19.00

Effect of Deformation Conditions on Grain Size and Microstructure Homogeneity of β-Rich Titanium Alloys

G.A. Salishchev, R.M. Galeyev, O.R. Valiakhmetov, M.F.X. Gigliotti, B.P. Bewlay, and C.U. Hardwicke

(Submitted August 24, 2005)

The mechanical behavior and microstructure evolution of a stable β, metastable β, and β-rich titanium alloys during hot deformation in both β and α/β phase fields were studied. The effects of thermomechanical processing and alloy content on final grain size and microstructure homogeneity in the alloys are given. The processing windows in both β and α/β phase fields for the formation of homogeneous microstructures with grain sizes down to submicron values are discussed. Isothermal multiple-step forging was used to produce the billets of a β-rich alloy with homogeneous fine-grained microstructure and low ultrasonic noise.

Keywords β-rich titanium alloy, microstructure homogeneity, ultrasonic noise

1. Introduction

Beta titanium alloys offer an attractive alternative to the α/β alloys due to their extended hot workability region arising from a lower β transus temperature (Ref 1). A high content of β-stabilizing elements impedes recovery/recrystallization processes and allows the easier formation of a microstructure with the smallest grain size in the β domain. As a result, the grain size in β titanium alloys after thermomechanical processing in the β phase field may be significantly smaller than that in the α/β alloys. The smaller the β grain size and the more homogeneous the microstructure after ingot breakdown in the β field, the lower are the strains required to form the homogeneous microstructure with the smallest grain size during hot working in the α/β field. Such a microstructure is very important not only for secondary processing, but also for ultrasonic inspectability. Ultrasonic inspectability is affected by microstructure: a microstructure containing acoustic entities with sizes comparable to the wavelength of the ultrasound exhibit high noise (Ref 2). So, it is necessary to control the regimes of thermomechanical processing to form at each processing stage the most homogeneous microstructure with the smallest grain size. The homogeneity of a recrystallized/globularized microstructure depends on the total strain and the uniformity of the strain distribution within the billet or forging. Therefore, to control microstructure and final properties the use of isothermal or near-isothermal deformation is required. Hot working temperatures for β titanium alloys have been defined for high strain rates, such as 10^{-1} to 10^{2} 1/s (where 1 is the original length), which are common for traditional processing techniques. At the same time, the microstructure evolution and mechanical behavior of β titanium alloys during low-strain-rate isothermal deformation have not been well studied until now.

The goal of the present work was to study the microstructure evolution and mechanical behavior of a stable β alloy, a metastable β alloy, and a β-rich alloy to define the parameters of thermomechanical processing needed to form a homogeneous microstructure with the smallest grain size and to produce a billet with reduced ultrasonic noise.

2. Experimental

Three alloys, stable βTi-33Mo, metastable βTi-11.4Mo-5.5Sn-4.2Zr, and β-rich Ti-17, were used. The alloys Ti-33Mo and Ti-11.4Mo-5.5Sn-4.2Zr were delivered by a Russian manufacturer, and Ti-17 was delivered by an American manufacturer. The chemical compositions and the β transus temperatures of the alloys are listed in Table 1. Hot-rolled rods that were 18 mm in diameter were used for the Ti-33 Mo and Ti-11.4Mo-5.5Sn-4.2Zr alloys. The Ti-17 alloy was a β-processed rod that was 203 mm in diameter and 1400 mm in length.

Tensile and compression tests were used for the study of the mechanical behavior of alloys. Strain rate sensitivity of flow stress (coefficient *m*) was determined by the strain rate-switching method. The mechanical properties of Ti-11.4Mo-5.5Sn-4.2Zr after hot deformation were studied by the compression of samples on a hydraulic press using an isothermal die unit. The samples were a-b-c forged with 50% strain at each step. The tensile samples were cut from those forgings.

The microstructure of deformed samples was studied using optical microscopy (OM) and transmission electron microscopy (TEM). The samples for microstructure analysis were cooled in water after deformation. The subgrain and grain sizes were estimated by OM and TEM techniques. Misorientations of the neighboring subgrains were determined using diffraction patterns.

This paper was presented at the Beta Titanium Alloys of the 00's Symposium sponsored by the Titanium Committee of TMS, held during the 2005 TMS Annual Meeting & Exhibition, February 13-16, 2005 in San Francisco, CA.

G.A. Salishchev, R.M. Galeyev, and **O.R. Valiakhmetov,** Institute for Metals Superplasticity Problems, Russian Academy of Sciences, Ufa, Russia; and **M.F.X. Gigliotti, B.P. Bewlay,** and **C.U. Hardwicke,** GE Research, Niskayuna, NY. Contact e-mail: canan.hardwicke@ge.com.

Table 1 Chemical composition of β titanium alloys

Alloy	Element content, wt.% (Ti – balance)											T_β, °C
	Al	Mo	Sn	Zr	Cr	Fe	Si	O	C	N	H	
VT30	…	11.4	5.5	4.2	…	0.08	0.07	0.10	0.015	0.012	0.010	745
Ti-33Mo	…	33	…	…	…	0.25	0.10	0.10	0.10	0.050	0.015	…
Ti-17	5.1	4.0	2.0	…	3.8	0.10	0.02	0.11	0.010	0.004	0.002	890

3. Results and Discussion

3.1 Mechanical Behavior and Microstructure Evolution of Ti-11.4Mo-5.5Sn-4.2Zr and Ti-33Mo during Deformation in the β Field

Figure 1 shows the temperature dependencies of the total elongation and the flow stress of both alloys at a strain rate of 1.3×10^{-3} s^{-1}. The stable Ti-33Mo alloy has much higher flow stresses compared with the metastable Ti-11.4Mo-5.5Sn-4.2Zr alloy. The latter alloy exhibited a higher decrease in the flow stress under transition to the β phase field. The changes in relative elongation with increasing temperature occurred in those alloys in accordance with changes in flow stress. But in the metastable alloy, elongation increased slightly upon increasing the temperature, while in the stable alloy a sharp increase in ductility occurred at temperatures higher than 900 °C.

Both alloys exhibited stress-strain dependencies that are typical for β titanium alloys (Fig. 2) (Ref 1). On the initial deformation stage, a peak of flow stress was observed, while further straining resulted in the steady-state flow stress. The lower the strain rate and the higher the deformation temperature, the lower the value of the peak flow stress.

Figure 3 shows the strain rate dependencies of the total elongation and flow stress for both alloys at different temperatures. With increasing strain rate, the ductility of the alloys decreased and the flow stress increased. The increase in the deformation temperature led to ductility improvement and to a decrease in the flow stress. The Ti-11.4Mo-5.5Sn-4.2Zr and Ti-33Mo alloys exhibited the features of superplasticity at 900 and 700 °C, respectively. In a certain strain-rate interval the strain-rate sensitivity of flow stress (coefficient m) is more than 0.3 (Fig. 3).

The distinction in the alloy composition did not lead to substantial differences in structure evolution during deformation. At the initial stage of deformation, the formation of subgranular structure and waviness of the grain boundaries was observed. The subgrain size increased by increasing the temperature or decreasing the strain rate. For both alloys, increasing the strain led to the formation of new grains at the initial grain boundaries, while subgrains were formed within the grain body. In the Ti-33Mo alloy, the subgrain and grain sizes were smaller than in the Ti-11.4Mo-5.5Sn-4.2Zr alloy (Table 2).

The microstructure evolution of Ti-11.4Mo-5.5Sn-4.2Zr deformed at 900 °C with a strain rate of 3.3×10^{-3} s^{-1} has been studied. At true strains between 0.7 and 1.0, a number of grains lost their contour due to recrystallization and polygonization (Fig. 4a). At higher strains, the microstructure remained unchanged. The subgrain size at strains of 1.1 and 1.4 was about 2 to 4 μm (i.e., almost no change compared with a strain of 0.7) (Table 2). Electron backscatter diffraction (EBSD) analysis revealed the increase in the fraction of high-angle grain boundaries during the deformation that testifies to the occurrence of recrystallization.

With increasing strain rate (>7×10^{-3} s^{-1}), the grains became elongated along the tensile direction. The straining was extremely nonuniform, and the increase in strain led to increasing microstructure heterogeneity. The deformation of the Ti-11.4Mo-5.5Sn-4.2Zr alloy at all temperatures in the β region resulted in similar changes in the microstructure.

Analysis of the deformation relief on the surface of polished samples of Ti-11.4Mo-5.5Sn-4.2Zr revealed that, along with the above-mentioned changes in the microstructure, displacement of grains occurs during deformation (Fig. 4b). The displacement of grains was not uniform; moreover, grain boundary sliding (GBS) did not develop in all grain boundaries. The contribution of GBS to the total mean straining of the alloy at 900 °C and a strain rate of ~6×10^{-3} s^{-1} (conditions corresponding to the maximum value of coefficient m) was estimated to be 35 ± 7%. The decrease in the strain rate to 1.4×10^{-4} s^{-1} led to a decrease in the contribution of GBS to 18 ± 4%.

The origin of the high ductility of the titanium alloy in the β region differs from that of conventional structural superplasticity. During hot deformation, the formation of subgrains occurs, and their misorientation increases up to medium- and high-angle boundaries. Their formation is a continuous process controlled by dynamic recovery. The forming grains and subgrains grow in the course of deformation. The new subboundaries form in them, and their misorientation increases, resulting in the formation of new grains. Therefore, the mean size of grains and subgrains at the steady-stress stage almost does not change. The formation of new grains at grain boundaries can occur as a result of bulging by the mechanism of discontinuous recrystallization.

Thus, the microstructure evolution observed during hot deformation is caused by the intense occurrence of dynamic recovery accompanied by the processes of dynamic recrystallization connected with the migration of grain and subgrain boundaries. Obviously, at certain temperatures and strain rate conditions, the optimal microstructure for superplasticity can be attained. Such a microstructure has the largest volume fraction of the new grains formed. This evidently increases the contribution of GBS to the total deformation.

The results show that the optimal parameters of thermomechanical processing should be determined by controlling the size of grains and subgrains, their shape, and uniformity. Therefore, the conditions of the isothermal deformation of alloys in the β phase field should be close to superplastic regimes.

Under certain temperatures and strain rate deformation conditions in the β phase field, the initial microstructure of both stable and metastable β alloys can be refined substantially. The microstructure formed is of a mixed character, combining recrystallized grains and a well-developed subgranular structure. Such a microstructure may be beneficial for secondary processing in the α/β field, resulting in an increase of the nucleation sites of the α phase and limiting the growth of α lamellas,

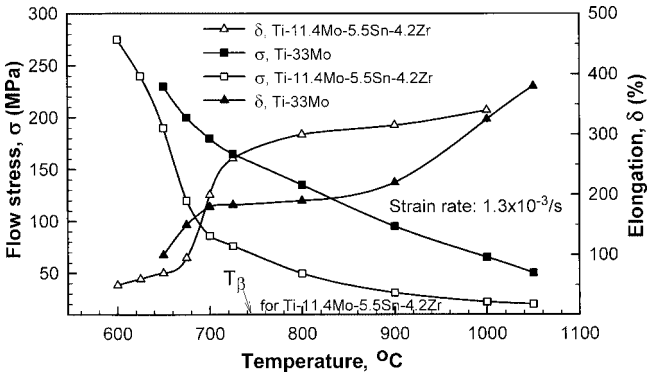

Fig. 1 Flow stress and elongation as a function of temperature for Ti-33Mo and Ti-11.4Mo-5.5Sn-4.2Zr alloys deformed at a strain rate of 1.3×10^{-3} s^{-1}

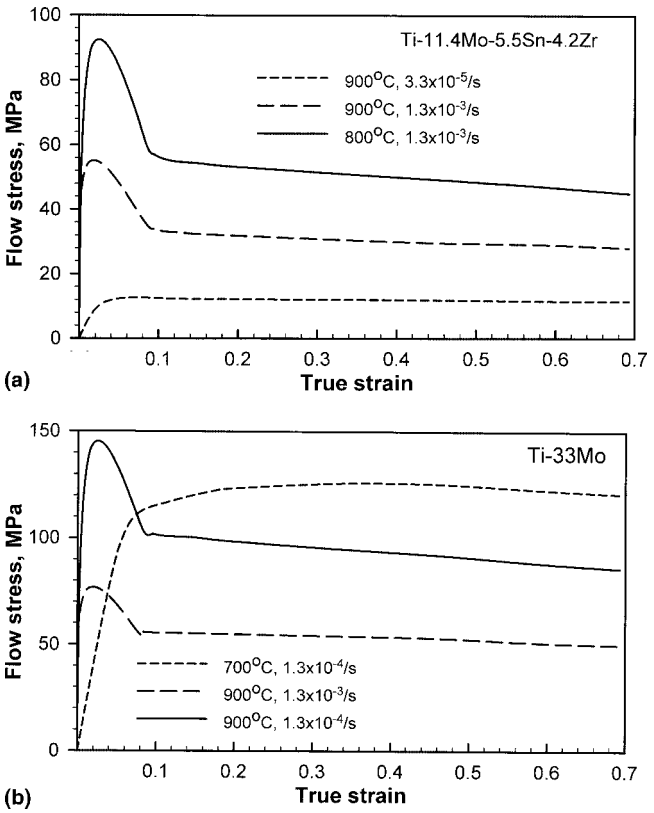

Fig. 2 Flow curves of (a) Ti-11.4Mo-5.5Sn-4.2Zr and (b) Ti-33Mo alloys

and, thus, leading to the formation of a homogeneous finely dispersed microstructure. Let us consider the influence of hot deformation on the microstructure and mechanical properties of the Ti-11.4Mo-5.5Sn-4.2Zr alloy, in which the decomposition of the metastable β phase in the course of deformation becomes more intense.

3.2 Mechanical Behavior and Microstructure Evolution of Ti-11.4Mo-5.5Sn-4.2Zr During Deformation in the α/β Field

The temperature dependencies of the flow stress and the total elongation for Ti-11.4Mo-5.5Sn-4.2Zr at a strain rate of

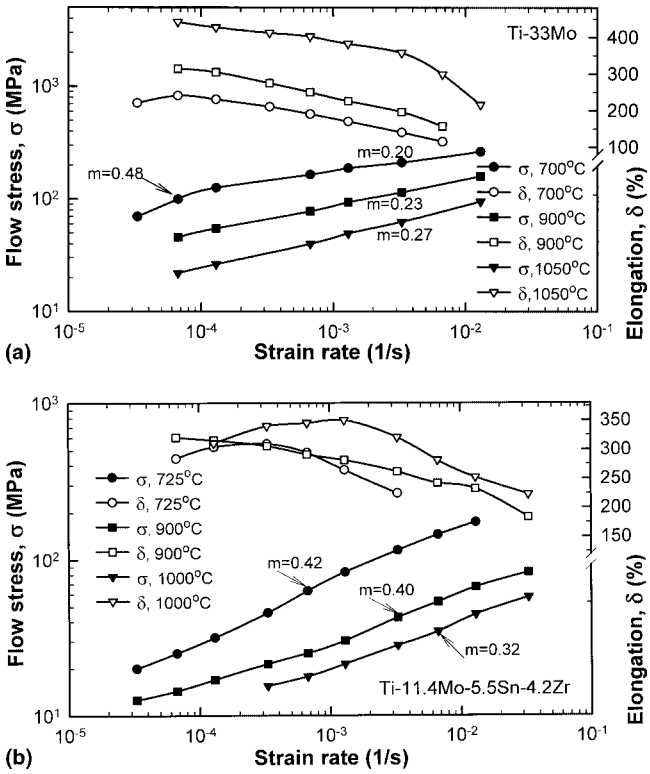

Fig. 3 Flow stress and elongation as a function of strain rate for (a) Ti-33Mo and (b) Ti-11.4Mo-5.5Sn-4.2Zr alloys

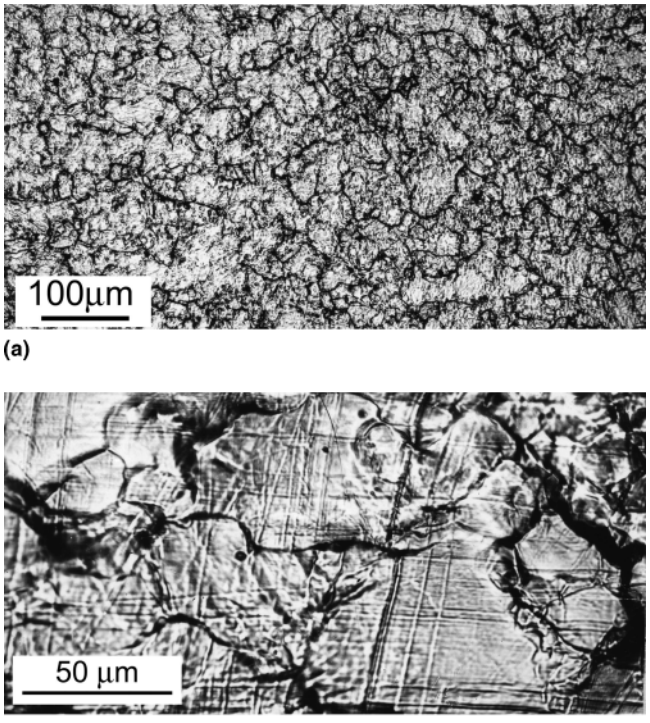

Fig. 4 Microstructure and deformation relief on the surface of the Ti-11.4Mo-5.5Sn-4.2Zr samples: (a) strained to $e \approx 1.0$ at 900 °C and 6.7×10^{-3} s^{-1}; (b) as a preliminary strained to $e \approx 0.8$, cooled to room temperature, polished and restrained to $e \approx 0.1$ at 900 °C and 6×10^{-3} s^{-1}

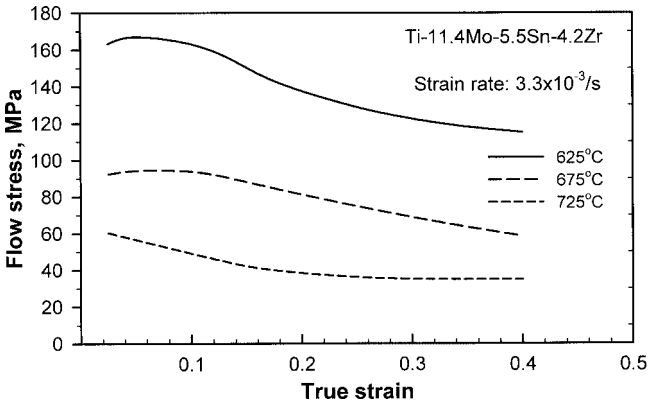

Fig. 5 Flow curves of the Ti-11.4Mo-5.5Sn-4.2Zr alloy deformed in an α/β field at strain rate of 3.3 to 10^{-5} s^{-1}

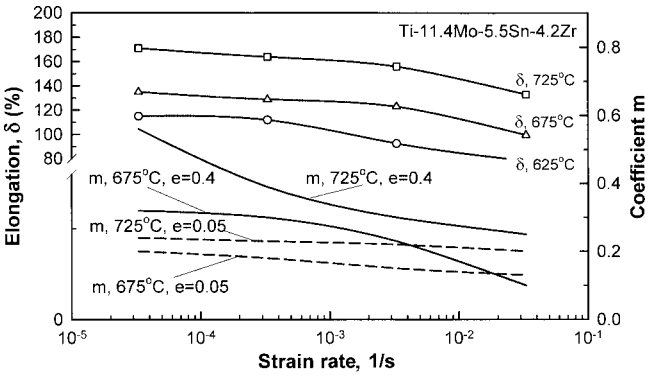

Fig. 6 Strain rate dependencies of total elongation and coefficient *m* for the Ti-11.4Mo-5.5Sn-4.2Zr alloy: dash line is coefficient *m* at $e = 0.05$; solid line, $e = 0.4$

Table 2 Dependence of structure parameters of β titanium alloys on strain rate

Alloy (temperature, true strain)	Average size of starting grains, μm	Strain rate, L/s	Size of recrystallized grains, μm	Size of subgrains, μm
Ti-11.4Mo-5.5Sn-4.2Zr (900 °C, $e \approx 0.7$)	80	3.3×10^{-5}	…	15-25
		3.3×10^{-4}	30-70	5-10
		3.3×10^{-3}	10-40	2-4
Ti-33Mo (700 °C, $e \approx 0.7$)	7	6.7×10^{-4}	1-2	0.2-0.7
		3.3×10^{-3}	0.2-0.5	≤0.1

1.3×10^{-3} s^{-1} are shown in Fig. 1. With an increased testing temperature, a decrease in flow stress and an increase in elongation were observed.

Figure 5 shows the stress-strain curves for the alloy within the temperature range of 625 to 725 °C. At the beginning of deformation, a peak stress was observed. The peak stress is reduced with increasing temperature and decreasing strain rate deformation. A further increase in strain led to flow softening.

Figure 6 shows the strain rate dependencies of the total elongation and coefficient *m*. With increasing strain rate, a decrease in the relative elongation value was observed at all temperatures. Elongation increased with the testing temperature within the strain rate range studied. The linear dependencies of the coefficient *m* on the strain rate at the initial stage of deformation ($e = 0.05$) at all temperatures were observed. After a true strain of 0.4, one could see the nonmonotone character of the strain rate dependence of the coefficient *m* and a considerable increase in its value. The highest elongation corresponded to maximum values of coefficient *m*. Thus, the results of mechanical tests showed that during the deformation of Ti-11.4Mo-5.5Sn-4.2Zr in the α/β phase field a transition to superplastic flow at a certain strains occurred.

Heating of the metastable Ti-11.4Mo-5.5Sn-4.2Zr alloy up to the testing temperature led to the β → α phase transformation. The dispersion of α plates forming and the volume fraction of the α phase depended on the heating temperature. So, at the temperature of 625 °C, the mean length of plates was 5 μm, and their mean thickness was 0.5 μm, while at 725 °C, the mean length was 15 μm and the mean thickness was 1 μm. Within the same temperature range during annealing for 0.5 h, the volume fraction of the α phase ranged from 20 to 8%. With increasing annealing time up to 2 h, the volume fraction of the α phase increased up to 30% at 625 °C and up to 12% at 725 °C.

The structure evolution of Ti-11.4Mo-5.5Sn-4.2Zr during hot deformation in the α/β field occurred due to several competitive processes, namely, dynamic recrystallization, phase transformation, and globularization. In areas of the β grains that were free of α plates, dynamic recrystallization was observed, which essentially depended on the β → α phase transformation during heating and deformation.

The microstructural homogeneity depended considerably on the deformation conditions (Table 3). The homogeneity was estimated from the volume fraction of the α phase particles preserving a lamellar-type shape after deformation and the volume fraction of the two phase areas.

During deformation, decomposition of the metastable β phase occurred and was accelerated by the stresses applied. For example, at 675 °C the volume fraction of the α phase was 15% before straining and about 35% after a true strain of 0.56. The formation of low- and high-angle grain boundaries in the β matrix during deformation contributes to the precipitation of dispersed α phase particles and their homogeneous distribution within the grain body. Due to the increase in the volume fraction of the α phase and the generation of particles within the β grain body, the microstructural homogeneity increased.

The phase transformation and recrystallization processes exerted effects on each other. The formation of the α phase particles within the β phase resulted in the redistribution of dislocations and the migration of subboundaries, and, thus, restricted the growth of subgrains and recrystallized β grains. Upon increasing the deformation temperature, the volume fraction of the α phase precipitates during heating and deformation decreased, and the distribution became nonhomogeneous. Moreover, in the single β phase, new recrystallized grains were formed, and their sizes were larger than those in the two-phase areas. As a result, the homogeneity of the microstructure decreased. In particular, at 725 °C and a strain rate of 3.3×10^{-4}

Table 3 Microstructure parameters for Ti-11.4Mo-5.5Sn-4.2Zr deformed to $e \approx 0.56$

Strain rate, L/s	Microstructure parameters at deformation temperature, °C								
	D_m, μm			*A*, %			*B*, %		
	625	675	725	625	675	725	625	675	725
3.3×10^{-5}	1/1	2/3	4/5	100	100	90	0	0	0
3.3×10^{-4}	0.5/0.5	1/1.2	2/5	97	93	80	5	0	0
3.3×10^{-3}	…	0.6/0.8	1.5/2	92	87	75	40	10	5
3.3×10^{-2}	…	0.5/0.5	1/1	85	80	70	70	50	20

Note: D_m, mean size of recrystallized grains (numerator, for α phase; denominator, for β phase); *A,* volume fraction of two-phase areas of struture; *B,* volume fraction of α particles preserving a lamellar type shape after deformation.

Table 4 Superplastic performance of Ti-11.4Mo-5.5Sn-4.2Zr with a SMC structure

Grain size, μm	Characteristics	Temperature, °C (strain rate ≈6×10^{-4}/s)							
		500	525	550	600	625	650	675	700
0.8	σ, MPa	…	…	…	238	98	53	49	47
	δ, %	…	…	…	250	580	610	610	370
	m	…	…	…	0.40	0.47	0.50	0.47	0.43
0.3	σ, MPa	567	472	130	90	…	…	…	…
	δ, %	55	85	390	430	…	…	…	…
	m	0.22	0.50	0.56	0.48	…	…	…	…

s^{-1} after straining to $e = 0.56$, the volume fraction of the α phase was found to be 14%, and the microstructure of the alloy contained two-phase areas with α and β grain sizes of 1 to 3 μm and single-phase areas with β grain sizes of 4 to 8 μm. With an increasing strain rate, the volume fraction of the α phase and the fraction of globular particles decreased simultaneously (Table 3), resulting in a decrease of the microstructure homogeneity at all of the temperatures studied.

The size of the recrystallized grains in the single-phase areas depended on the temperature and strain rate conditions of deformation, becoming smaller with decreasing temperature and/or increasing strain rate. At the same time in the two-phase areas the grain size depended not only on the deformation conditions but also on the volume fraction and dispersion of the α phase precipitates. The increase in the volume fraction of the α phase particles and their dispersion was responsible for grain size refinement and improvement in microstructure homogeneity. In the Ti-11.4Mo-5.5Sn-4.2Zr alloy, a submicrocrystalline (SMC) structure with a grain size less than 1 μm was formed at temperatures below 650 °C (Table 3).

The study of mechanical properties of the samples cut from the Ti-11.4Mo-5.5Sn-4.2Zr billets, preliminarily subjected to compression at 650 °C and a strain rate of 10^{-4} s^{-1}, revealed superplastic behavior within the wide temperature range (Table 4). The features of superplastic flow were observed even at rather low temperatures for the titanium alloy, namely, at 600 °C.

It should be noted that the formation of the SMC structure essentially expands the temperature range of superplasticity toward low temperatures. In particular, values for the strain rate sensitivity coefficient *m* ranging from 0.4 to 0.5 were observed within the temperature interval of 600 to 725 °C. The highest superplastic properties were observed within the range of 650 to 675 °C, where $\sigma = 50$ MPa and $\delta = 610\%$ (Table 4). At the same time, similar to the analogous titanium alloy Beta III (composition: 11.0mass%Mo-6.4mass% Zr-4.3mass%Sn; $T_\beta = 745$ °C) with a grain size of 8 μm, the same level of superplastic characteristics was observed only at higher temperatures of 704 to 730 °C and lower strain rates of 6×10^{-5} s^{-1}) (Ref 3).

So, the formation of the homogeneous microstructure in the Ti-11.4Mo-5.5Sn-4.2Zr alloy during hot deformation in the α/β field essentially depends on the relationship of the dynamic recrystallization of the β phase, the phase transformation, and globularization. The kinetic correlation between them, which can be achieved at certain temperature-strain rate conditions close to superplastic deformation, may lead to the formation of highly homogeneous microstructure with the smallest grain size. The results of the current study revealed that the most homogeneous fine-grained microstructure is formed in Ti-11.4Mo-5.5Sn-4.2Zr alloy within the temperature range of 625 to 675 °C and at strain rates of 3.3×10^{-5} to 3.3×10^{-4} s^{-1}. In this case, the true strain value should be no less than 0.4 to 0.6.

3.3 Ti-17 Alloy Billet Processing for Low Ultrasonic Noise

From an ultrasonic inspectability perspective, titanium material with a regulated fine-grain microstructure has an advantage: it has lower ultrasonic noise. For α/β titanium alloys, acoustic scattering arises from colonies of α particles sharing a common crystallographic *c*-axis (Ref 2, 4). Alpha/beta titanium alloy billets can be produced with microstructures that are substantially free of crystallographic texture at grain sizes less than approximately 10 μm (Ref 4, 5). Such a homogeneous globular microstucture is formed, for instance, by multiaxial forging in the α/β phase field under conditions of temperature, strain, and strain rate for dynamic recrystallization/globularization and superplasticity (Ref 5, 6). Let us consider the possibility of the formation of a microstructure providing low levels of backscattered ultrasonic noise in the β-rich Ti-17 alloy.

3.4 Procedure Development of Pilot Process for Ti-17 Fine Grain Billets

The macrostructure and microstructure of the cross section of the as-received Ti-17 billet are shown in Fig. 7. The micro-

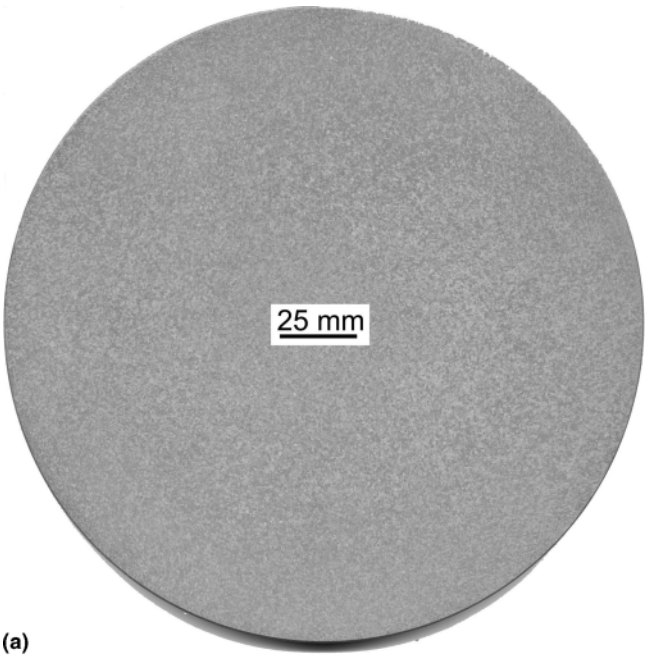

(a)

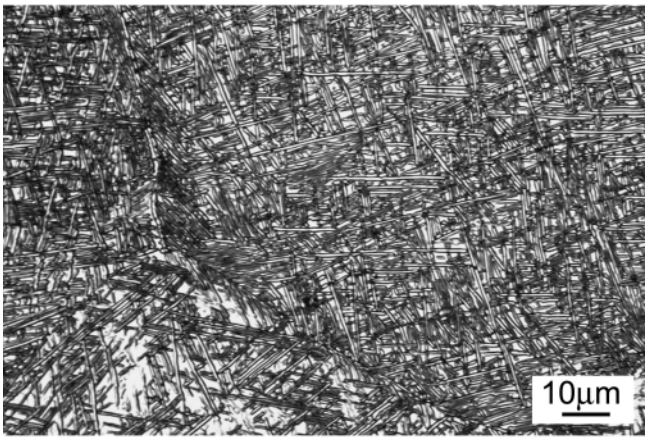

(b)

Fig. 7 Macrostructure (a) and microstructure (b) of as-received Ti-17 billet

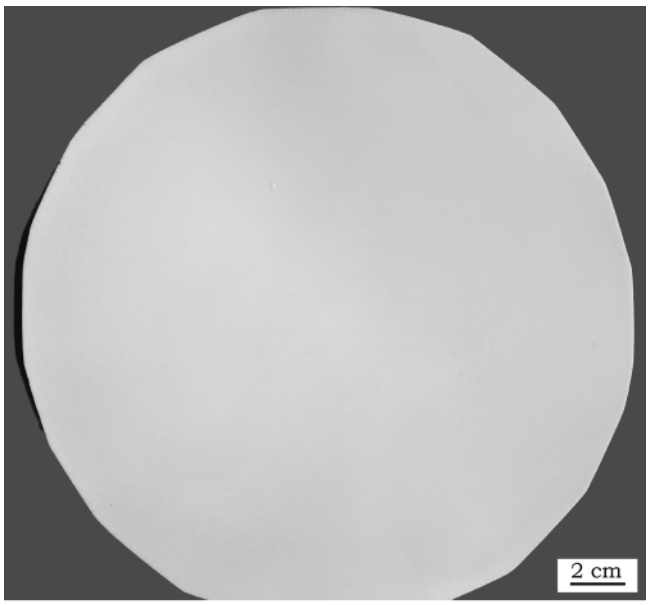

(a)

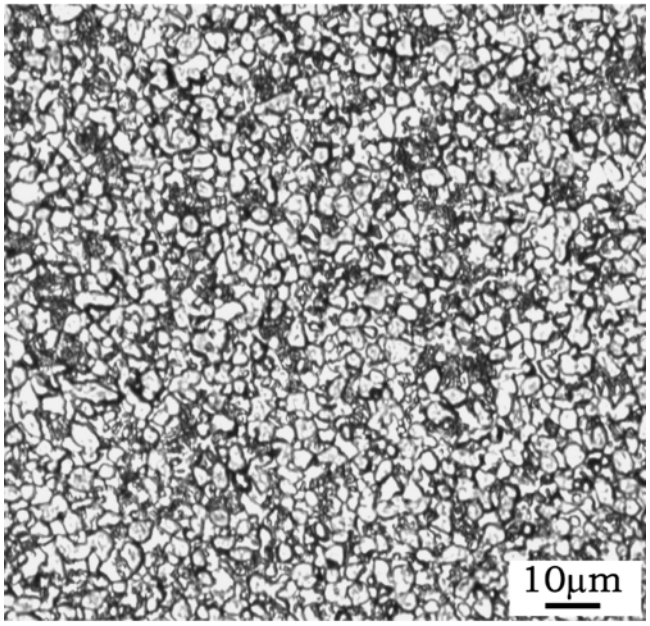

(b)

Fig. 8 Macrostructure (a) and microstructure (b) of ultra-fine-grain Ti-17 billet

structure has the coarse-grained lamellar structure. Fine and short plates of α phase are present inside the matrix β grains. The β grain size ranged from 0.5 to 1 mm, and the thickness and length of the α plates ranged from 1 to 2 μm and 10 to 20 μm, respectively.

To determine the temperature range for the thermomechanical processing of alloy Ti-17 for a fine-grained microstructure, the samples in the as-received condition were compressed at 760, 800, and 845 °C at a strain rate of ~10^{-3} s^{-1}. The average α grain size in the microstructure of samples deformed to 65% strain decreased with decreasing deformation temperature and was about 4, 3, and 1.5 μm for deformation temperatures 845, 800, and 760 °C, respectively. Based on the results obtained, a procedure was developed for producing billets of Ti-17 having a globular microstructure with a grain size ranging from 4 to 8 μm. It included the a-b-c-forging in the temperature range from 800 to 850 °C and strain rates between 10^{-3} and 10^{-4} s^{-1}.

A cross section of the uniform fine-grained (UFG) Ti-17 billet at a distance equal to a quarter of the billet length is shown in Fig. 8(a); the macrostructure of the billet is homogeneous and has a dull surface. The microstructure of the fine-grain processed Ti-17 is shown in Fig. 8(b) with a globular microstructure consisting of 4 to 8 μm grains.

3.5 Electron Backscatter Diffraction Analysis

Samples of a β-processed billet and samples from the fine-grain processed Ti-17 material were analyzed by EBSD. For the images of orientation shown in Fig. 9, shades of gray represent distinct crystallographic orientation, white represents the other phase, and black represents regions the phase and/or orientation of which could not be determined.

With reference to Fig. 9(a), the α phase appears to be fine

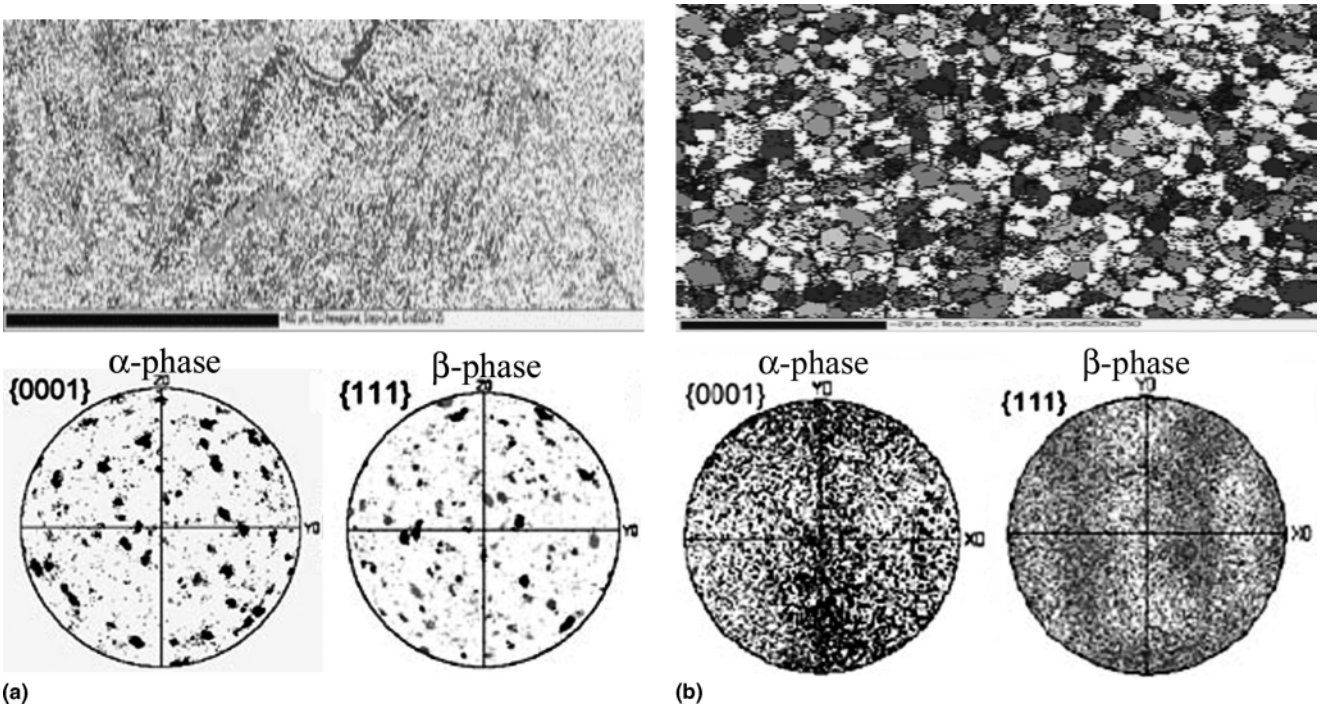

Fig. 9 EBSD images and pole figures from (a) conventionally processed and (b) fine grained-processed Ti-17

scale and with random crystallographic orientation, but the β phase is representative of large grains. The analysis of the pole figures for the α and β phases has shown that there are only a few unique sets of poles for the β phase, which is consistent with only a few β grains. In contrast, the α phase has many *c*-axis orientations, which is consistent with all variants of the Burgers relationship present in each grain. With reference to Fig. 9(b), both the α and β phases exhibit random crystallographic orientation and are less than 10 μm in diameter. There are about equal amounts of the α and β phases. For the pole figures of either phase (α and β), there are large numbers of unique orientations, which is consistent with the research objective to produce a UFG structure.

3.6 Ultrasonic Evaluation

Ultrasonic C-scans were conducted on blocks of titanium alloy billet material at 5 and 10 MHz. The blocks were 38 mm tall, and most contained nine flat-bottom holes that were machined to within 13 mm of the top surface. The flat-bottom holes were 0.8 mm in diameter. Two scans were conducted at each frequency to determine signal to noise. One scan was adjusted to record ultrasonic reflections from within the block, a measure of ultrasonic noise; a second scan was adjusted to record the reflections from the flat-bottom holes, a measure of a signal from a flaw. A block was machined from conventionally processed Ti-17 billet as well as from a block of the same alloy in the UFG-processed condition. Additionally, there was a cylinder of fused silica. The results of ultrasonic C-scans are presented as the signal-to-noise ratio illustrated in Fig. 10 in comparison with those for titanium alloys Ti64 and Ti6242 in conventionally processed and UFG-processed conditions (Ref 2, 5).

As seen in Fig. 10, the conventionally processed material has higher ultrasonic noise and lower signals from flat-bottom holes than do those corresponding UFG-processed material.

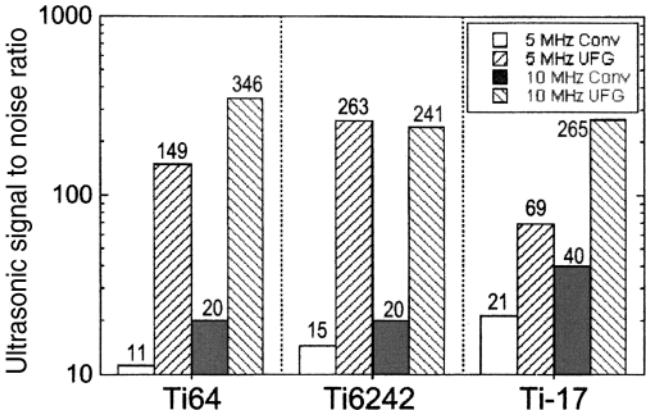

Fig. 10 Signal-to-noise from a 0.8 mm diameter flat-bottom hole in Ti alloy blocks

4. Summary

The evolution of the β microstructure during the hot deformation of β titanium alloys is caused by the occurrence of dynamic recovery and recrystallization. At certain temperatures and strain rate intervals of isothermal deformation, a microstructure suitable for superplastic flow can be formed, and thus, the regimes of thermomechanical treatment of alloys should be close to superplastic conditions.

The formation of the homogeneous globular-type microstructure in metastable β and β-rich alloys depends considerably on the kinetic correlation among the processes of dynamic recrystallization/globularization, phase transformation, and superplasticity occurring in the α/β phase field. A highly homogeneous fine-grained microstructure with grain sizes down to submicron values can be also formed under thermomechanical conditions close to superplastic deformation.

Processing to produce UFG microstructures possessing random crystallographic orientations of grains of both the α and β phases in the billets of β titanium alloys has been defined. Uniform fine grain-processed billets have ultrasonic transparency advantages.

References

1. I. Weiss and S.L. Semiatin, Thermomechanical Processing of Beta Titanium Alloys: An Overview, *Mater. Sci. Eng. A,* Vol 243, 1998, p 46-65
2. M.F.X. Gigliotti, B.P. Bewlay, J.B. Deaton, R.S. Gilmore, and G.A. Salishchev, Microstructure-Ultrasonic Inspectability Relationships in Ti6242: Signal-to-Noise in Fine-Grain-Processed Ti6242, *Metall. Mater. Trans. A,* Vol 31, 2000, p 2119-2125
3. F.H. Froes, C.F. Yolton, J.C. Chesnutt, and C.H. Hamilton, Microstructure Control in Titanium Alloys for Superplastic Behavior, *Forging and Properties of Aerospace Materials,* 1978, Metals Society, London, p 371-398
4. M.F.X. Gigliotti, B.P. Bewlay, C.U. Hardwicke, R.S. Gilmore, G.A. Salishchev, R.M. Galeyev, and O.R. Valiakhmetov, "Uniform Fine-Grain Processing of α-β Titanium Alloys," presented at Thermec'00: Processing and Manufacturing of Advanced Materials (Las Vegas, NV), T. Chandra, K. Higashi, C. Suryanarayana, and C. Tome, Ed., December 4-8, 2000
5. G.A. Salishchev, R.M. Galeyev, O.R. Valiakhmetov, S.V. Zherebtsov, M.F.X. Gigliotti, and B.P. Bewlay, Fine-Grained Billet Processing of Titanium Alloys, *Titanium'99: Science and Technology,* Vol II, I.V. Gorynin and S.S. Ushkov, Ed., CRISM Prometey, 2000, p 1563-1568
6. G.A. Salishchev, O.R. Valiakhmetov, and R.M. Galeyev, Formation of Submicrocrystalline Structure in the Titanium Alloy VT8 and Its Influence on Mechanical Properties, *J. Mater. Sci.,* Vol 28, 1993, p 2898-2902